

1 ***Klebsiella pneumoniae* BolA contributes to cell morphology, siderophore
2 production, stresses challenge, cell adhesion and virulence**

3 Xiangjin Yan,^a Feiyang Zhang,^a Manlin Ding,^a Li Xiang,^a Jiawei Bai,^a Qin Li,^a
4 Yingshun Zhou,^{a*#}

5 ^aDepartment of Pathogenic Biology, School of Basic Medicine, Southwest Medical
6 University, Luzhou, Sichuan, China

7 #Address correspondence to yingshunzhou@swmu.edu.cn.

8 *Present address: Yingshun Zhou, Southwest Medical University, Luzhou, Sichuan,
9 China.

10 **ABSTRACT** *Klebsiella pneumoniae* infection is one of the important reasons for the
11 increased of morbidity and mortality. The main virulence factors of *K. pneumoniae*
12 include capsule polysaccharide, lipopolysaccharide, fimbriae, outer membrane
13 proteins and siderophores. BolA homologues form a broadly conserved family of
14 proteins in prokaryotes and eukaryotes. In *Escherichia coli*, *bolA* expression is
15 quickly induced in response to different stresses or stationary phase that rapidly
16 adapt to changing environments. In this report, we confirmed that *bolA* mutant
17 strain exhibited increased sensitivity to bile and oxidative stresses. In addition, gene
18 deletion showed that *bolA* has an important role for the adherence of *K. pneumoniae*
19 to host cell and establishment in mice, including liver, spleen, kidney and lung
20 tissues, and induce the formation of liver abscess in mice. Our results also
21 demonstrated that *K. pneumoniae* *bolA* increases the production of siderophore and

22 virulence in *Galleria mellonella* larvae. Collectively, our results demonstrated that *K.*
23 *pneumoniae* **BolA** is a new virulence factor which contributes to survival in different
24 stresses and overcome host defense. These findings are helpful for the research of
25 new treatment strategies for *K. pneumoniae* infection.

26

27 **IMPORTANCE** *Klebsiella pneumoniae* is an important conditional pathogen causing
28 nosocomial infections and community-acquired infections. It can resistant to
29 multiple antibiotics, causing refractory infections and public health threat.
30 Therefore, new treatments are required to fight the pathogen, and a better
31 understanding of its virulence factors are needed to develop new drugs. Here, we
32 unraveled the role of BolA in survival under different stresses and overcome host
33 defense. Our results suggested that *bolA* actively contributes to cell morphology,
34 stresses challenge, cell adhesion and siderophore production that are tightly related
35 to bacterial virulence. Therefore, *bolA* mutant strain reduces the virulence of *K.*
36 *pneumoniae* in *G. mellonella* larvae and its colonization ability in mice. These results
37 reported *bolA* is a key virulence factor in *K. pneumoniae*, and they are helpful for
38 research of new therapies to treat this increasingly problematic pathogen.

39 **KEYWORDS** *bolA*, *Klebsiella pneumoniae*, stresses challenge, virulence, colonization

40 *Klebsiella pneumoniae* is an opportunistic pathogen that causes community infections
41 and hospital infections^[1-3]. It has the ability to metastasize spread, as well as extremely
42 high morbidity and mortality^[4, 5]. *K. pneumoniae* is classified into two types: classical

43 *Klebsiella pneumoniae* (CKP) mainly occurs in hospitals and long-term-care facilities,
44 while hypervirulent *Klebsiella pneumoniae* (hvKP) causes community-acquired,
45 tissue-invasive *K. pneumoniae* infections in otherwise healthy individuals that often
46 presented in a variety of sites^[6]. These cases included severe pneumonia, urinary tract
47 infection (UTI), sepsis, pyogenic liver abscess (PLA), endophthalmitis, meningitis and
48 necrotizing fasciitis^[4, 7-9]. *K. pneumoniae* ubiquitous in the environment and is often
49 found in the gastrointestinal tract and on medical devices^[10, 11]. The loss of porins,
50 overexpression of efflux pumps, the prevalence of carbapenemases and
51 extended-spectrum β-lactamases often lead to the emergence of multidrug-resistant *K.*
52 *pneumoniae*, causing a variety of refractory infections^{[6][12-14]}. Therefore, in order to
53 combat these daunting infections, it is necessary to identification of critical virulence
54 factors in *K. pneumoniae*.

55 Environmental stresses can induce adaptive responses of bacteria cells to ensure
56 survival, which is often related to virulence^[15, 16]. Stress response protein BolA was first
57 discovered in *E. coli*, and its homologues form a broadly conserved family of proteins in
58 prokaryotes and eukaryotes^[17]. In *E. coli*, it was discovered that *bolA* can make cells
59 shorter and thicker after a period of starvation or stationary phase conditions, and the
60 ability of bacteria to perception and adapt to harsh environmental conditions is critical to
61 survival^[18]. Later, it was found that the expression of *bolA* was affected by growth-rate,
62 *bolA* induced expression during the transition from exponential phase to stationary phase
63 due to the depletion of nutrients^[19]. At the exponential phase, *bolA* expression is quickly

64 induced in response to several stresses, such as sudden carbon starvation, osmotic stress,
65 acidic stress, heat stress or oxidative stress, allowing the bacteria to quickly adapt to harsh
66 environmental conditions^[20]. In addition, *bolA* has an essential role in the regulation of
67 cell permeability^[21] and biofilm formation^[22, 23]. In recent years, further studies have
68 found that BolA is a bacterial transcription factor, that elevated levels of BolA can induce
69 tricarboxylic acid (TCA) cycle genes, fimbria-like adhesins-related genes and repression
70 of flagellum-associated genes with consequences for bacterial motility and biofilm
71 formation^[24]. It also participates in the expression of DGCs and PDEs, which affects the
72 synthesis and degradation of secondary signal metabolite c-di-GMP^[25]. These studies
73 prompted us to research the effect of transcription factor BolA on the virulence of *K.*
74 *pneumoniae*.

75 *K. pneumoniae* have multiple virulence factors including lipopolysaccharide, capsule
76 polysaccharide, outer membrane proteins, fimbriae, nitrogen source utilization and
77 siderophores, for survival and immune evasion during infection^[9]. It is worth noting that
78 *K. pneumoniae* iron uptake genes are associated with capsule formation,
79 Hypermucoviscosity (HMV), purulent tissue infection and are found in invasive strains^[26].
80 In the present work, we identified a *bolA* homolog in *K. pneumoniae* NTUH-K2044 and
81 unravel its role in several phenotypes associated with the process of cell morphology,
82 siderophore production, cell adhesion, tissue colonization, liver abscesses and virulence.

83 **RESULTS**

84 **BolA is required for *K. pneumoniae* cell morphology and siderophore production**

85 To search for homologs of *K. pneumoniae* BolA, the *E. coli* K-12 W3110 amino acid
86 sequence (GenBank accession no. APC50728.1), *S. Typhimurium* SL1344 amino acid
87 sequence (GenBank accession no. FQ312003.1) and *K. pneumoniae* NTUH-K2044 amino
88 acid sequence (Laboratory sequencing results) were used. The amino acid sequences of
89 *bolA* in *K. pneumoniae* and *E. coli* are 91.4% similarity, and that of *S. Typhimurium*
90 SL1344 was 91.4% (data not shown). Moreover, the predicted 3D structures of BolA
91 proteins are nearly identical for the three species, (Fig. 1A). *K. pneumoniae* and *E. coli*
92 BolA protein have a $\alpha_1\beta_1\beta_2\alpha_2\alpha_3\beta_3\alpha_4$ fold with four α -helices and three β -sheets (Fig.
93 1B). We have used a virulent *K. pneumoniae* strain (NTUH-K2044) to construct a *bolA*
94 mutant strain and complementation strain. Scanning electron microscopy of these cells
95 revealed some effects of *bolA* on cell morphology (Fig. 1C). During exponential phase in
96 LB medium, wild type (WT) cells exhibited the classical rod-shaped morphology, and
97 during stationary phase in LB medium, WT cells exhibited shorter and wider morphology,
98 but the Δ *bolA* cells were generally longer and thinner than the WT cells, and similar to
99 WT cells shape during exponential phase. Moreover, the results of transcriptome
100 sequencing showed that the "transport" genes were significantly enriched in GO
101 enrichment analysis. And siderophores are an important virulence factor in *K.*
102 *pneumonia*^[27]. Therefore, we were interested in using CAS plate to detect the
103 siderophores of *K. pneumoniae*. The WT strain exhibited a larger orange halo than *bolA*

104 mutant strain (Fig. 1D). The *bolA* deletion reduced the area of the orange halo about 2.6
105 times that of the WT strain (Fig. 1E). This result suggests that the delete of the *bolA* gene
106 reduces the production of siderophore. Next, we investigated whether *K. pneumoniae*
107 *bolA* affects biofilm formation. Using a 96-well plate model, our results showed that the
108 biofilm biomass of *bolA* mutant strain was significantly lower than WT strain (Fig. 1F),
109 suggesting that *bolA* is required for *K. pneumoniae* biofilm formation.

110 **BolA is an important bacterial transcription factor in *K. pneumoniae***

111 To evaluate the impact of *K. pneumoniae* BolA in global transcriptional regulation.
112 Transcriptome sequencing was performed to compare the transcriptomic profiles of the
113 WT and Δ *bolA* strains; 146 differentially expressed genes were revealed between these
114 two strains in stationary phase. Of these differentially expressed genes, 26 were
115 upregulated and 120 were downregulated. Most differentially expressed genes were
116 distributed in downregulated.

117 Software GOseq based on Wallonia's non-central hyper-geometric distribution were
118 performed on the groups of genes significantly upregulated or downregulated. Among
119 them, the down-regulated differentially expressed genes are mainly enriched in T2SS and
120 T6SS, these two secretion systems are important virulence factors for bacteria. Gene
121 Ontology (GO) enrichment analysis showed differentially expressed genes involved in
122 membrane, localization, transport, oxidoreductase, tRNA processing (Fig. 2B). Kyoto
123 Encyclopedia of Genes and Genomes (KEGG) enrichment analysis indicated

124 differentially expressed genes involved in metabolism, transporters and secretion system
125 (Fig. 2C). Stress response protein BolA was confirmed to be induced during the transition
126 into stationary phase^[19, 28]. It is interesting to observe that the genes in *bolA* mutant strain
127 are downregulated during stationary phase, including several genes associated with
128 secretion system *gspK*、*gspF*、*gspE*、*clpV(TssH)* and *VgrG*. More surprisingly, several
129 genes associated with transport including *livF*、*livH*、*ydeY*、*KP1_3194*、*FbpB*
130 (*KP1_3174*)、*fecD*、*FhuB* (*KP1_1440*)、*potC*、*potB*、*afuB*、*afuA*、*kdpB* and *kdpA* are
131 downregulated (table 1) during stationary phase, in which *FhuB*、*fecD*、*FbpB*、
132 *KP1_3194*、*afuB* and *afuA* genes are directly related to the iron transport. BolA also
133 promotes the expression of several biofilm-related genes (*mhpB*, *ydeY*, *iold*) and
134 oxidoreduction-related genes (*ulaA*, *KP1_4425*, *KP1_1420*, *KP1_2565*).
135 **BolA is an important metabolic modulator of *K. pneumoniae***

136 To compare the differentially accumulated metabolites between WT and Δ *bolA* strains,
137 LC-MS was used for metabolite identification. In total, 82 differentially accumulated
138 metabolites with known specific substances were screened. These differentially
139 accumulated metabolites were defined as those with a variable importance for projection
140 (VIP) value >1 , P value <0.05 compared to WT. Among the detected metabolites, 25
141 metabolites were upregulated, and 57 metabolites were downregulated. Among them, 17
142 metabolites were increased, and 24 metabolites were decreased in pos mode, while 8
143 metabolites were increased, and 33 metabolites were decreased in neg mode. The

144 differentially accumulated metabolites were visualized by volcano map (Fig. 3A).

145 After metabolomic analysis, five metabolites related to stress resistance and virulence
146 were identified, which were Agmatine, Cadaverine, Guanosine, Flavin adenine
147 dinucleotide (FAD) and D-biotin respectively (table 2). It is speculated that the
148 downregulation may be the factor leading to the weakening of the virulence and stress
149 resistance of the *bolA* mutant strain of *K. pneumoniae*.

150 In order to validate these results, the expression of several of these genes were further
151 analyzed by qPCR (Fig. 3B). Twelve different genes were selected for analysis, including
152 the differentially expressed genes mentioned above and ppGpp synthetic-related genes.
153 The regulation pattern of these genes is consistent with the transcriptome analysis results,
154 and these genes are downregulated after *bolA* deletion.

155 **BolA promotes *K. pneumoniae* survival in bile and oxidative stresses**

156 To evaluate the role of *K. pneumoniae* *bolA* in intestinal colonization, bacteria
157 underwent specific intestinal stresses associated with osmotic, bile and oxidative. For the
158 osmotic resistance assay, no significant difference was observed between the *K.*
159 *pneumoniae* NTUH-K2044 and *bolA* mutant strains in LB medium containing 0.5M of
160 NaCl (Fig. 4A). In bile challenge experiment, we were examined the ability of the strains
161 to tolerate bile in LB medium, and significant difference was observed between the WT
162 and Δ *bolA* strains (Fig. 4B). WT, Δ *bolA* and complementation strains were growth in LB

163 medium containing 1% of ox bile, the ability of WT strain to grow in the 1% bile was
164 three-fold higher than Δ bolA strain, and complementation strain restored the ability to
165 tolerate bile stress. Oxidative stress assay showed that the Δ bolA strain had 1.79-fold
166 greater sensitivity to 30% H₂O₂ (inhibition zone =13.73 cm²) than the WT strain
167 (inhibition zone =7.69cm²) (Fig. 4C). Collectively, these results suggest that the response
168 of the bolA in *K. pneumoniae* in bile, and oxidative stresses.

169 **BolA promotes *K. pneumoniae* cell adhesion and colonization of mice**

170 The WT and Δ bolA strains were compared for their ability to adhere to HCT116 human
171 colon cancer cells (Fig. 6). The bolA mutant strain was significantly decreased adherence
172 compared with the WT strain, mounting 2.8fold lesser adherence to HCT116 cells. Next,
173 we performed in vivo verification. We used a mouse septicemia infection model to
174 observe the colonization of bacteria in mouse tissues Including the liver, spleen, lung and
175 kidney. Ten-week-old female BALB/c mice were intraperitoneally injected with 2×10^4
176 CFU in 500 μ L of NS. The mice were euthanized at 24h postinoculation (hpi) and the liver,
177 spleen, lung and kidney bacterial burdens were determined. Given transcription factor
178 bolA deletion, we anticipated that the mutant strain would be attenuated, and this was
179 indeed observed. We found that the colonization ability of *K. pneumoniae* in liver, spleen,
180 lung and kidney tissues of mice after the bolA deletion was significantly lower than the
181 WT strain. In the liver, spleen, lung and kidney at 24 hpi, the Δ bolA strain had
182 colonization levels about 4 logs lower than *K. pneumoniae* NTUH-K2044 (Fig. 6B).

183 These data indicated that the *bolA* mutant strain ability to survive and spread was
184 attenuated in the mice.

185 Histopathological evaluation of the livers from WT-infected mice at 120 hours after
186 infection revealed the frequent presence of either macroabscesses (Fig. 7C, arrow) or
187 large abscesses (Fig. 7F, arrow). The high-power field (magnification, $\times 40$) shows the
188 microabscesses composed of inflammatory cells (Fig. 7D, arrow). In contrast, no liver
189 abscesses were observed in Δ *bolA*-infected mice (Fig. 7E). The numbers of liver
190 abscesses were 14, 17, 12, 3 (mean, 11.5) in 4 WT-infected mice, and 0, 0, 0, 0 (mean, 0)
191 in 4 Δ *bolA*-infected mice (WT vs Δ *bolA*, $P < 0.01$; Student t test). Moreover, In
192 WT-infected mice, gross liver abscesses were observed (Fig. 7A, arrow). In conclusion, *K.*
193 *pneumoniae* BolA can obviously induce the formation of multiple liver abscesses in mice.

194 **The BolA promotes *K. pneumoniae* virulence**

195 To evaluate the involvement of *bolA* in virulence, we used the *G. mellonella* larvae for
196 *K. pneumoniae* infection^[29]. *G. mellonella* larvae were injected with PBS or 2×10^5
197 CFU/larva of the *K. pneumoniae* NUTH-K2044 WT, Δ *bolA* or complementation strains,
198 and the survival rate was daily monitored over a period of 72 hours. The results of
199 infection by the WT strain were clearly seen at 72 hours of infection, with a decrease of
200 about 83% of the initial larvae population (Fig. 6A). It's worth noting that the *bolA*
201 mutant strain was found to increase by 53% the larval survival rate at 72h of infection

202 compared with the survival rate of the WT strain (Fig. 6A). Complementation of the *bolA*
203 mutant strain was shown to majority restore the virulence to WT levels (Fig. 6A). These
204 results clearly indicate the essential role of *bolA* in the pathogenesis of *K. pneumoniae* in
205 the *G. mellonella* larvae infection model.

206 **DISCUSSION**

207 In this paper, we characterized the *K. pneumoniae* NUTH-K2044 BolA protein. The
208 BolA protein is highly conserved among *E. coli*, *K. pneumoniae* and *S. typhimurium*. In *E.*
209 *coli*, when bacteria enter the stationary phase or under harsh environmental conditions,
210 the *bolA* will be overexpressed to make the bacterial cells become rounder and shorter to
211 protect the bacteria^[30]. We saw the same results in *K. pneumoniae*. The cell morphology
212 of the *bolA* mutant strain during stationary phase cannot be rounder and shorter like the
213 WT strain. The shorter and rounder of bacterial cells result in a decrease in surface to
214 volume ratio, and thus less surface area exposed to the damaging or unfavourable
215 environments. This is consistent with previous research that overexpression of *bolA*
216 induces formation of spherical cells in *E. coli*^[20]. Growth analyses revealed that the
217 deletion of *bolA* in *E. coli* was reported to increase the growth rate compared to the WT
218 strain in a nutrient-rich medium (LB medium)^[17]. However, the deletion of *bolA* in *S.*
219 *Typhimurium* strain (SL1344) did not significantly affect the growth rate relative to the
220 WT strain^[28]. In *K. pneumoniae* NTUH-K2044, while different, *bolA* mutant strain did
221 not significantly impact the growth rate relative to the WT strain, and only a slight

222 increase in the optical density at 595nm of the *bolA* mutant strain at the end of the
223 exponent phase and the value of OD₅₉₅ a slight decrease at the stationary phase was
224 observed. However, in M9 medium, growth analyses of *bolA* mutant and WT strains
225 revealed that the *bolA* deletion significantly reduced the growth rate and terminal density
226 at 595nm (see Fig. S1). In addition, the researchers have found that the importance of
227 accurate regulation of cross-talk between second messenger c-di-GMP and *bolA* for a
228 proper response in the regulation of biofilm development^[25]. Therefore, we also
229 conducted biofilm formation experiments and MIC assays. While, *bolA* did not impact
230 the MIC level (see Table S1). And the ability of biofilm formation of *bolA* mutant strain
231 was significantly lower than WT strain, which is consistent with previous studies^[31].
232 These results providing additional evidence that *bolA* plays distinct roles in these
233 organisms.

234 BolA is a bacterial transcription factor that directly binds to the promoter region of a
235 number of important genes, *fhlD*, *fliA*, *gltA*, and *mreBCD*^[31]. Several studies have
236 indicated the critical contribution of transcriptional regulators in bacterial adaptation and
237 virulence^[32-36]. These studies emphasize the significance of the identification of new
238 transcriptional regulators to understand and overcome *K. pneumoniae* pathogenesis
239 strategies. In *E. coli*, BolA is a stress response protein whose expression increases under
240 imposition of diverse severe conditions, conferring protection to the cells^[37]. The deletion
241 of *bolA* in *S. Typhimurium* was reported to increased survival under acid and oxidative

242 stress compared to WT strain^[28]. Furthermore, *bolA* expression is quickly induced in
243 response to several stresses, such as sudden carbon starvation, osmotic stress, acidic
244 stress, heat stress or oxidative stress, allowing the bacteria to quickly adapt to
245 environmental changes at the log phase^[20]. Above all, we suggested that BolA is a
246 virulence factor that overexpresses itself in hostile environments to protect to the cells.
247 These facts prompted us to research the effect of transcription factor BolA on the
248 virulence capacity of *K. pneumoniae*. Unsurprisingly, our findings suggest that the
249 response of *K. pneumoniae* *bolA* gene in bile, and oxidative stresses and increases its
250 viability under both stresses. Our research also found that the deletion of *bolA* in *K.*
251 *pneumoniae* significantly reduce its adhesion rate in intestinal cells HCT116. These
252 studies point to a possible role of *bolA* in *K. pneumoniae* virulence capacity.

253 Interestingly, some results have showed that transcription factor BolA affects different
254 pathways directly related to virulence^[17, 31]. Iron is an essential nutrient for the host and
255 most microorganisms^[38]. Microorganisms produce siderophore which is a small molecule
256 of iron chelators and is an important virulence factor and whose main function is to iron
257 uptake from the host and provide this essential metal nutrient to microorganisms^[4, 39].
258 Moreover, two characteristics known to distinguish CKP from hvKP strains are the
259 number of siderophore iron acquisition systems and the abundance of capsules^[8].
260 Classical strains usually have one or two siderophore iron acquisition systems, while HV
261 strains have three or four, and HV strains produced very thick capsular and showed a high

262 mucinous viscosity (HMV). In this study, transcriptome data and qPCR suggested *BolA*
263 direct effects are related to the induction of genes related with the iron transport. So, we
264 carried out CAS agar plate experiment and found that *bolA* has a positive regulatory
265 effect on siderophore production. The results of research show that the *bolA* mutant strain
266 exhibited litter halo than WT strain in a CAS ager plate. So far, this is the first time we
267 have identified the role of *bolA* in capacity of Iron uptake. We hypothesized that *bolA*
268 affects the production of siderophore by regulating iron transport-related genes.

269 In the field of infection biology, *G. mellonella* larvae are becoming an attractive
270 infection model for human pathogens. *G. mellonella* larvae can grow at 37°C, so the
271 model of larvae is more suitable for the study of human pathogenic bacteria. And it has
272 innated immune like that of mammals' response to infections. In *G. mellonella* larvae
273 killing experiment, our results suggest that the delete of the *bolA* gene significantly
274 reduced the virulence of *K. pneumoniae* in the larva of *G. mellonella*. The results showed
275 that *K. pneumoniae* *bolA* gene was absent and the pathogenicity of the bacteria was
276 decrease, similar to what was observed for the *S. Typhimurium* *bolA* homolog^[28].

277 In addition to *bolA* effect on cell morphology, growth rate in M9 medium, resistance to
278 bile and oxidation also influenced its capacity to colonize in mice and induced the
279 formation of liver abscess in mice. In *V. cholera*, *ibaG* is a *bolA* gene's homologue. Very
280 recently, we have shown that the deletion of *ibaG* in *V. cholera* exhibited obvious
281 colonization defects in intestinal tract colonization. When stationary-phase cultures were

282 used to infect mice, the *ibaG* mutant strain showed 50-fold deficit in colonization
283 compared with WT strain inoculated^[40]. Thus, we hypothesized that the *bolA* deletion
284 significantly reduced the ability to colonize the liver, lung, spleen and kidney organs of
285 mice. Not surprisingly, we observed the same results for the first time, showed that *bolA*
286 induced the formation of multiple microabscesses and large abscesses in mice liver tissue.
287 Its ability to adhere to the intestinal epithelium is attenuated. Adhesion to intestinal
288 epithelial could happen in the earlier stage of infection, seem to be important for *K.*
289 *pneumoniae* pathogenesis. Histopathological examination revealed that the deletion of
290 *bolA* in *K. pneumoniae* exhibited a lack of ability to induce liver abscess. These data
291 indicate that *bolA* is essential for *K. pneumoniae* to survive, colonize, which contributes
292 to liver abscess generation and host death. We hypothesized these are related to that the
293 *bolA* mutant strain is associated with decreased colonization ability in the host and
294 reduced the ability of bacteria cells to protect themselves in the host.

295 Transcriptome results showed that the expression of T2SS, T6SS and iron
296 absorption-related virulence genes of the Δ *bolA* strain were significantly down-regulated.
297 In addition, the metabolome results showed that related to virulence and stress resistance
298 of the Δ *bolA* strain metabolites (including biotin, spermine, cadaverine, guanosine, and
299 FAD) were downregulated. And the results of qPCR tests showed that the expression of
300 T2SS, T6SS, iron transport and ppGpp synthetic related genes were downregulated after
301 *bolA* was deleted, the results of transcriptome sequencing were consistent. It is worth

302 noting that guanosine can become c-di-GMP when phosphorylated. Furthermore,
303 c-di-GMP and ppGpp are second messenger of bacteria that plays an important role in
304 signal transduction. C-di-GMP can regulate a variety of biological pathways. Previous
305 studies have found that the increase in the level of c-di-GMP has a significant inhibitory
306 effect on the movement of *Pseudomonas aeruginosa*, positively regulates the formation
307 of biofilms and the production of siderophore, and improve resistance to oxidative
308 stress^[41]. The ppGpp has a variety of physiological functions, the most important of
309 which is to coordinate the stress response of bacteria to stress, and the RelA/SpoT
310 homologous protein is a key protein that regulates the level of ppGpp^[42]. Therefore, we
311 hypothesized that virulence factor BolA may promotes the virulence of *K. pneumoniae* by
312 promoting the accumulation of five metabolites (including biotin, spermine, cadaverine,
313 guanosine, and FAD) and the expression of genes related to T2SS, T6SS, iron transport
314 and ppGpp synthesis.

315 In order to investigate the different roles of *bolA* of *K. pneumoniae*, we tested the
316 different strains of iron uptake, M9 medium and LB medium to growth rate, the adhesion
317 of different strains to intestinal cells HCT116, their resistance to bile, osmotic and
318 oxidative stress, as well as the ability of killing *G. mellonella* larvae. Finally, the
319 colonization ability of different strains in liver, lung, spleen and kidney tissues of mice
320 and the role of *bolA* in liver abscess formation were tested by mice septicemia infection
321 model. Taken together, we demonstrate, for the first time, that *K. pneumoniae* virulence

322 factor BolA has important regulatory roles in bacterial morphology, biofilm formation
323 and production of siderophore and virulence. In particular, the *bolA* gene was deleted,
324 which reduced bile and oxidative stress resistance and reduced liver, spleen, lung and
325 kidney colonization in mice. This study show that virulence factor BolA is a good
326 candidate as a therapeutic target against *K. pneumoniae* systemic infection.

327 **MATERIALS AND METHODS**

328 **Bacterial strains, plasmids, primers, and growth conditions.**

329 The bacterial strains and plasmids used in the present work are listed (see Table S2).
330 All the primers used in this study are listed in Table 2. All bacterial strains were stored at
331 -80°C in lysogeny broth (LB) medium containing 25% glycerol. pkO3-Km was used to
332 create gene mutant strain by homologous recombination. Unless otherwise stated, *K.*
333 *pneumoniae* and *E. coli* cultures were grown in LB medium, M9 medium or on LB ager
334 at 30°C, 37°C or 43°C and supplemented with Kanamycin (Km, 50µg/ml or 25µg/ml)
335 where required. Bacterial growth was monitored by measuring the optical density at
336 595nm.

337 **Construction of the *bolA* gene deletion and complementation strains.**

338 A *bolA* gene deletion strain of *K. pneumoniae* NTUH-K2044 strain was constructed
339 with the previously described method^[43]. In brief, the left and right flanking DNA
340 fragments of *bolA* gene were amplified by overlap PCR and cloned into pKO3-Km by

341 digested, ligated, and then introduced into NTUH-K2044 by electroporation. To construct
342 the complementation strain ($\Delta bolA+bolA$ strain), the DNA fragment that contained the
343 *bolA* coding sequence and promoter region (using primers *bolA-HB-F/R*) (see Table S3)
344 was amplified by PCR. Then, the DNA fragment was cloned into the pGEM-T-easy-km.
345 After, the recombinant plasmid was transformed in $\Delta bolA$ strain by electroporation. The
346 gene deletion mutant and complementation strains were verified by PCR and sequence
347 determination.

348 **Scanning electron microscopy.**

349 The supernatants were discarded after bacterial cultures were centrifuged. Bacterial
350 cells were overnight fixed at 4°C in 2.5% glutaraldehyde. Followed by washing them
351 three times with PBS, and then dehydrated by gradient incubation, and finally anhydrous
352 ethanol was used for suspension. Drops of the bacterial suspension were applied to a
353 glass coverslip, dried, and covered with chromium. Finally, bacterial cells were observed
354 and photographed.

355 **CAS agar assays for iron uptake.**

356 A chrome azurol S (CAS) agar assays were performed as previously described^[44, 45]. In
357 brief, 60 ml of CAS solution was first prepared by dissolving 60.5 mg CAS powder
358 (Yuanye Bio-Technology, China) was added to 50 ml of double-distilled water (ddH₂O),
359 followed by 10 ml of 1 mM solution of FeCl₃ (Aladdin) was added. Then, 72.9 mg

360 hexadecyltrimethylammonium bromide (HDTMA; Yuanye Bio-Technology, China) was
361 added in 40 ml ddH₂O. At last, a 100 ml CAS stock solution was made by HDTMA
362 solution was poured slowly with stirring into CAS solution and autoclaved to sterilize.
363 Next, the freshly autoclaved 1.5% agar LB plate and CAS stock solution were mixed at a
364 ratio of 9:1 to make A CAS agar plate. then, 2 μ l overnight bacterial culture (WT and
365 Δ bolA strains) was inoculated to the CAS plate and cultivated at 28°C. The CAS plate
366 was photographed after 48h of cultivation. The assay was repeated three times.

367 **Transcriptome sequencing.**

368 Overnight cultures were diluted 1:100 in fresh LB medium. Bacterial cultures were
369 collected at stationary-phase. Then, the cells were harvested to extract total RNA. The
370 total RNA was extracted, the quality of the RNA samples was detected, and Illumina
371 sequencing was performed at Novogene Bioinformatics Technology Co., Ltd (Beijing,
372 China).

373 **Assay Metabolome.**

374 Overnight cultures were centrifuged at 8000g for 10 minutes at 4°C. The supernatants
375 were discarded; cell pellets were washed three times in 10 mL of PBS (4°C) and
376 resuspended in an extraction solvent consisting of methanol/water (4:1 v/v), and a 6 mm
377 grinding bead was added. After grinding for 6 minutes with a frozen tissue grinding
378 instrument, the sample was extracted with low temperature ultrasound for 30 minutes,

379 and then the sample was placed at -20°C for 30 minutes The supernatant was centrifuged
380 for 15 minutes and transferred to a tube for analysis. The sample extracts were analyzed
381 using an (Liquid chromatography mass spectrometry) LC-MS system, and the data were
382 analyzed on the free online platform of Majorbio Cloud Platform.

383 **qPCR assays**

384 WT and *bolA* mutant strains were grown in LB medium to stationary phase, then and
385 bacterial cells were collected. The total RNA was extracted from harvested cells with
386 Spin Column Bacteria Total RNA Purification Kit (Sangon Biotech). The cDNA was
387 synthesized using TransScript® All-in-One First-Strand cDNA Synthesis SuperMix for
388 qPCR (One-Step gDNA Removal). All qPCR assays were performed at least three times
389 using Tip Green qPCR SuperMix (TransGen Biotech). The primers used for qPCR are
390 shown (see Table S3). The data were analyzed by the $\Delta\Delta CT$ method using 16S mRNA as
391 an internal control. Fold change was calculated using the $\Delta\Delta CT$ method. All qPCR
392 reactions were performed in triplicate.

393 **Minimum Inhibitory Concentration (MIC) assays.**

394 MIC assays were performed by micro-dilution broth method in 96-well microplates. In
395 short, bacterial cultures in exponential phase were diluted to a final OD₅₉₅ of 0.1, then
396 diluting it 1,000-fold into fresh LB medium. Next, 100 μ L of microbial suspension was
397 added into each well and 100 μ L of antimicrobial agents were added only in the first well.

398 From the first well, serial twofold dilutions of the antimicrobial agents were done and the
399 plates were incubated without shaking for 24 h at 37°C. *E. coli* ATCC 25922 was used as
400 a reference strain (control).

401 **Biofilm assays.**

402 The overnight cultures of bacteria were diluted to a final optical density OD₅₉₅ of 0.1 in
403 fresh LB medium. Then, 200µl of the diluted cultures were added to a 96-well
404 Polystyrene (PS) plate and incubated at 37°C for 48 h. Bacterial cells were washed twice
405 with ddH₂O to remove plankton, and the attached bacteria were stained with 0.1% crystal
406 violet for 10 minutes. Finally, the plate was washed four times with ddH₂O. The crystal
407 violet was solubilized by anhydrous ethanol, and the biofilm thickness was estimated by
408 measuring the OD₅₉₅ values.

409 **Stresses challenge assays.**

410 Bile, osmotic stresses assays were performed based on a previously described
411 method^[46]. Briefly, bacterial cultures were grown separately until they reached an OD₅₉₅
412 of 0.2 in LB medium. Then, cultures were spread plated onto LB agar plates containing
413 NaCl (0.25M, 0.5 M, 0.75M) and bile (1.0%, Sangon Biotech) respectively. The plates
414 were incubated overnight at 37°C, and the numbers of colonies were counted. The results
415 are expressed as the ratio of the number of colonies obtained from LB agar plate
416 containing NaCl or bile to the number of colonies obtained from LB agar plate. These

417 experiments were performed at least three times.

418 For oxidative stress sensitivity assays, the exponential-phase bacterial cultures were
419 diluted to an OD₅₉₅ of 0.2 and were uniformly spread over an LB agar plate. Then, a
420 sterile 6-mm paper disk (5 μ l of 30% H₂O₂) was placed at the center on the agar surface.
421 Next, The plates were incubated at 37°C for 24 h. The experiments were repeated at least
422 three times.

423 **Adherence assays.**

424 HCT116 human colon cancer cells were grown in RPMI 1640 medium supplemented
425 with 10% fetal bovine serum (FBS), 100 U/ml penicillin, and 0.1 mg/ml streptomycin^[47].
426 Cells adhesion assays were performed mainly according to the methods described
427 previously with minor modifications^[48, 49]. For adherence experiments, HCT116 cells
428 were grown to confluent monolayers in 24-well plates, and then the cells were washed
429 twice with HBSS. Followed by 200 μ l of *K. pneumoniae* cells (OD₅₉₅, 0.5) in FBS-free
430 RPMI 1640 medium were added to each well and were settled onto host cells by
431 centrifugation at 200 \times g for 5 minutes. After 1h of incubation in a humidified 5% CO₂
432 mosphere at 37°C, cells were washed 4 times with PBS and then bacteria were released
433 by the addition of 0.5% Triton X-100. Recovered bacteria were quantified by means of
434 serial dilution and plating onto LB agar. The experiment was performed at thrice.

435 **G. mellonella larvae killing assays.**

436 G. mellonella larvae killing assays were performed as described previously^[50]. In brief,
437 *K. pneumoniae* strains were prepared by harvesting exponential phase bacterial cultures,
438 washing twice in PBS and then adjusting to 1×10^7 CFU. Groups of larvae (N = 10) were
439 injected with 10 μ l of working bacterial suspension at the last proleg using a hypodermic
440 microsyringe. For each assay, a group of larvae was injected with PBS as a control.
441 Injected larvae were placed in petri dishes at 37°C for 72h in the dark. The percent
442 survival was recorded at 24h intervals. G. mellonella larvae were considered dead if they
443 did not respond to physical stimuli. Assays were repeated at three times.

444 **Mice infection experiments.**

445 Ten-week-old female BALB/c mice (n=5 in each group) were used for infections.
446 Bacterial cells were collected by centrifugation and resuspended in sterile normal saline
447 (NS). Mice were infected by intraperitoneal injection of the bacterial suspension (1×10^4
448 CFU *K. pneumoniae*/mouse). After 24h, the mice were euthanized and organs (including
449 liver, spleen, kidney, lung) were homogenized in NS, and then appropriate dilutions were
450 plated onto LB agar for CFU counts.

451 Eight-week-old female BALB/c mice (4 per group) were infected by intraperitoneal
452 injection with *K. pneumoniae* at a dose of 2×10^3 CFUs per mouse for 120 hours. The
453 livers were retrieved, fixed in 10% formalin, and embedded in paraffin blocks. The tissue
454 sections were stained with hematoxylin-eosin and were imaged and quantified under a
455 light microscope. The number of abscesses was quantified in five low-power fields
456 (magnification, $\times 4$).

457 **Statistical analyses.**

458 All statistical analysis was performed using Prism (GraphPad). *G. mellonella* larvae
459 survival was calculated by means of Kaplan-Meier analysis with a log-rank (Mantel-Cox)
460 test. Differences in *K. pneumoniae* burden in tissues between groups were examined
461 based on unpaired nonparametric Mann-Whitney U tests. Adherence assays, stresses
462 challenge assays and iron uptake assays were analyzed by t test. Statistically significant
463 was defined by $P < 0.05$ (*), $P < 0.01$ (**), $P < 0.001$ (***), and $P < 0.0001$ (****).

464 **ACKNOWLEDGMENTS**

465 This research was funded by the National Natural Science Foundation of China
466 [31500114] and the Sichuan Province Science and Technology project [2020YJ0338].

467 **REFERENCES**

- 468 [1] Wen-Chien K. Community-Acquired Klebsiella pneumoniae Bacteremia: Global Differences in Clinical Patterns [J].
469 Emerging Infectious Diseases, 2002, 8(2): 160-6.
- 470 [2] Moradigaravand D, Martin V, Peacock S J, et al. Evolution and Epidemiology of Multidrug-Resistant Klebsiella
471 pneumoniae in the United Kingdom and Ireland [J]. mBio, 2017,
- 472 [3] Holt K E, Wertheim H, Zadoks R N, et al. Genomic analysis of diversity, population structure, virulence, and
473 antimicrobial resistance in *Klebsiella pneumoniae*, an urgent threat to public health [J]. Proceedings of the
474 National Academy of Sciences, 2015, 112(27): E3574-E81.
- 475 [4] Paczosa M K, Mecsas J. Klebsiella pneumoniae: Going on the Offense with a Strong Defense [J]. Microbiology &
476 Molecular Biology Reviews Mmbr, 2016, 80(3): 629.
- 477 [5] Chew K L, Lin R T P, Teo J W P. Klebsiella pneumoniae in Singapore: Hypervirulent Infections and the
478 Carbapenemase Threat [J]. Front Cell Infect Microbiol, 2017, 7(515).
- 479 [6] Russo T A, Olson R, Fang C T, et al. Identification of biomarkers for the differentiation of hypervirulent Klebsiella
480 pneumoniae from classical *K. pneumoniae* [J]. Journal of Clinical Microbiology, 2018, 56(9): JCM.00776-18.
- 481 [7] Lee H C, Chuang Y C, Yu W L, et al. Clinical implications of hypermucoviscosity phenotype in Klebsiella
482 pneumoniae isolates: association with invasive syndrome in patients with community-acquired bacteraemia [J].
483 Journal of Internal Medicine, 2010, 259(6): 606-14.
- 484 [8] Shon A S, Bajwa R P S, Russo T A. Hypervirulent (hypermucoviscous) Klebsiella pneumoniae: a new and
485 dangerous breed [J]. Virulence, 2013, 4(2): 107-18.

486 [9] Li B, Zhao Y, Liu C, et al. Molecular pathogenesis of *Klebsiella pneumoniae* [J]. Future Microbiology, 2014, 9(9):
487 1071-81.

488 [10] Clegg S, Murphy C N. Epidemiology and Virulence of *Klebsiella pneumoniae* [J]. Microbiol Spectr, 2016, 4(1):

489 [11] Richard S. Nosocomial klebsiella infections: intestinal colonization as a reservoir [J]. Annals of Internal Medicine,
490 1971, 74(5): 657-64.

491 [12] None. Success of an infection control program to reduce the spread of carbapenem-resistant *Klebsiella*
492 *pneumoniae* [J]. Infection Control & Hospital Epidemiology, 2009, 30(5): 447-52.

493 [13] Li J, Zhang H, Ning J, et al. The nature and epidemiology of OqxAB, a multidrug efflux pump [J]. Antimicrobial
494 Resistance & Infection Control, 2019, 8(1):

495 [14] Wand M E, Jamshidi S, Bock L J, et al. SmvA is an important efflux pump for cationic biocides in *Klebsiella*
496 *pneumoniae* and other Enterobacteriaceae [J]. Scientific Reports, 2019, 9(1):

497 [15] Srinivasan V B, Mondal A, Venkataramaiah M, et al. Role of oxyRKP, a novel LysR-family transcriptional regulator,
498 in antimicrobial resistance and virulence in *Klebsiella pneumoniae* [J]. Microbiology (Reading, England), 2013, 159(Pt
499 7): 1301-14.

500 [16] Fàbrega A, Vila J. *Salmonella enterica* serovar *Typhimurium* skills to succeed in the host: virulence and regulation
501 [J]. Clin Microbiol Rev, 2013, 26(2): 308-41.

502 [17] Guinote I B, Moreira R N, Barahona S, et al. Breaking through the stress barrier: the role of BolA in
503 Gram-negative survival [J]. World Journal of Microbiology & Biotechnology, 2014, 30(10): 2559-66.

504 [18] Aldea M, Hernández-Chico C, De La Campa A G, et al. Identification, cloning, and expression of bolA, an
505 ftsZ-dependent morphogene of *Escherichia coli* [J]. Journal of bacteriology, 1988, 170(11): 5169-76.

506 [19] Aldea M, Garrido T, Hernández-Chico C, et al. Induction of a growth-phase-dependent promoter triggers
507 transcription of bolA, an *Escherichia coli* morphogene [J]. Embo Journal, 8(12): 3923-31.

508 [20] Santos J M, Freire P, Vicente M, et al. The stationary-phase morphogene bolA from *Escherichia coli* is induced by
509 stress during early stages of growth [J]. Molecular Microbiology, 1999, 32(4): 789-98.

510 [21] Patrick F, Vieira H L A, Furtado A R, et al. Effect of the morphogene bolA on the permeability of the *Escherichia*
511 *coli* outer membrane [J]. Fems Microbiology Letters, 1): 106-11.

512 [22] Vieira H L A, Freire P, Arraiano C M. Effect of *Escherichia coli* morphogene bolA on biofilms [J]. Applied &
513 Environmental Microbiology, 2004, 70(9): 5682-4.

514 [23] Birgit K, Ole N. Initial characterization of a bolA homologue from *Pseudomonas fluorescens* indicates different
515 roles for BolA-like proteins in *P. fluorescens* and *Escherichia coli* [J]. Fems Microbiology Letters, 1): 48-56.

516 [24] Clémentine, Dressaire, Ricardo, et al. BolA Is a Transcriptional Switch That Turns Off Motility and Turns On
517 Biofilm Development [J]. mBio, 2015,

518 [25] Moreira R N, Dressaire C, Barahona S, et al. BolA Is Required for the Accurate Regulation of c-di-GMP, a Central
519 Player in Biofilm Formation [J]. Mbio, 2017, 8(5): e00443-17.

520 [26] Remya P A, Shanthi M, Sekar U. Characterisation of virulence genes associated with pathogenicity in *Klebsiella*
521 *pneumoniae* [J]. Indian journal of medical microbiology, 2019, 37(2): 210-8.

522 [27] Barbosa V a A, Lery L M S. Insights into *Klebsiella pneumoniae* type VI secretion system transcriptional regulation
523 [J]. BMC Genomics, 2019,

524 [28] Mil-Homens D, Barahona S, Moreira R N, et al. Stress Response Protein BolA Influences Fitness and Promotes
525 *Salmonella enterica* Serovar *Typhimurium* Virulence [J]. Applied and environmental microbiology, 2018, 84(8):

526 [29] Insua J L, Llobet E, Moranta D, et al. Modeling *Klebsiella pneumoniae* Pathogenesis by Infection of the Wax Moth
527 *Galleria mellonella* [J]. *Infection and immunity*, 2013, 81(10): 3552-65.

528 [30] Santos J M, Freire P, Vicente M, et al. The stationary-phase morphogene *bolA* from *Escherichia coli* is induced by
529 stress during early stages of growth [J]. *Molecular Microbiology*, 2010, 32(4): 789-98.

530 [31] Clémentine D, Ricardo Neves M, Susana B, et al. *BolA* is a transcriptional switch that turns off motility and turns
531 on biofilm development [J]. *Mbio*, 2015, 6(1): 02352-14.

532 [32] Storey D, Mcnally A, Strand M, et al. *Klebsiella pneumoniae* type VI secretion system-mediated microbial
533 competition is *PhoPQ* controlled and reactive oxygen species dependent [J]. *PLoS pathogens*, 2020, 16(3): e1007969.

534 [33] Dan P, Xuan L, Pin L, et al. Transcriptional regulation of *galF* by *RcsAB* affects capsular polysaccharide formation
535 in *Klebsiella pneumoniae* NTUH-K2044 [J]. *Microbiological Research*, 2018, S0944501318302453-.

536 [34] Disi L, Jinming F, Jingjie W, et al. The Fructose-Specific Phosphotransferase System of *Klebsiella pneumoniae* Is
537 Regulated by Global Regulator CRP and Linked to Virulence and Growth [J]. *Infection & Immunity*, 2018, IAI.00340-18-.

538 [35] Wu C C, Wang C K, Chen Y C, et al. *IscR* regulation of capsular polysaccharide biosynthesis and iron-acquisition
539 systems in *Klebsiella pneumoniae* CG43 [J]. *PLoS One*, 2014, 9(9): e107812.

540 [36] Lin C T, Wu C C, Chen Y S, et al. *IscR* Regulation of Capsular Polysaccharide Biosynthesis and Iron-Acquisition
541 Systems in *Klebsiella pneumoniae* CG43 [J]. *Microbiology*, 2011, 157(Pt 2): 419-29.

542 [37] Guinote I B, Moreira... R N. Breaking through the stress barrier: the role of *BolA* in Gram-negative survival [J].
543 *World Journal of Microbiology & Biotechnology*, 30(10): 2559-66.

544 [38] Cassat J E, Skaar E P. Iron in Infection and Immunity [J]. *Cell Host & Microbe*, 13(5): 509-19.

545 [39] Behnsen J, Raffatellu M. Siderophores: More than Stealing Iron [J]. *Mbio*, 7(6): e01906-16.

546 [40] Fleurie A, Zoued A, Alvarez L, et al. A *Vibrio cholerae* *BolA*-Like Protein Is Required for Proper Cell Shape and Cell
547 Envelope Integrity [J]. *mBio*, 2019, 10(4):

548 [41] Wang T, Cai Z, Shao X, et al. Pleiotropic Effects of c-di-GMP Content in *Pseudomonas syringae* [J]. *Applied and*
549 *environmental microbiology*, 2019, 85(10):

550 [42] Hauryliuk V, Atkinson G C, Murakami K S, et al. Recent functional insights into the role of (p)ppGpp in bacterial
551 physiology [J]. *Nature reviews Microbiology*, 2015, 13(5): 298-309.

552 [43] Hsieh P F. Serum-Induced Iron-Acquisition Systems and *TonB* Contribute to Virulence in *Klebsiella pneumoniae*
553 Causing Primary Pyogenic Liver Abscess [J]. *Journal of Infectious Diseases*, 2008, 197(12): p.1717-27.

554 [44] Tingting, Wang, Zhao, et al. Pleiotropic Effects of c-di-GMP Content in *Pseudomonas syringae* [J]. *Applied &*
555 *Environmental Microbiology*, 2019,

556 [45] Owen J G, Ackerley D F. Characterization of pyoverdine and achromobactin in *Pseudomonas syringae* pv.
557 *phaseolicola* 1448a [J]. *Bmc Microbiology*, 2011, 11(

558 [46] Bharathi S V, Vasanth V, Amitabha M, et al. Role of the Two Component Signal Transduction System *CpxAR* in
559 Conferring Cefepime and Chloramphenicol Resistance in *Klebsiella pneumoniae* NTUH-K2044 [J]. *Plos One*, 2012, 7(4):
560 e33777.

561 [47] Guillaume L B, Jean-Félix S, Philippe G, et al. The NAG Sensor *NagC* Regulates LEE Gene Expression and
562 Contributes to Gut Colonization by *Escherichia coli* O157:H7 [J]. *Frontiers in Cellular & Infection Microbiology*, 2017, 7(

563 [48] Chun-Ru, Hsu, Yi-Jiun, et al. *Klebsiella pneumoniae* Translocates across the Intestinal Epithelium via Rho GTPase-
564 and Phosphatidylinositol 3-Kinase/Akt-Dependent Cell Invasion [J]. *Infection & Immunity*, 2014,

565 [49] Sahly H, Podschun R, Oelschlaeger T A, et al. Capsule impedes adhesion to and invasion of epithelial cells by
566 *Klebsiella pneumoniae* [J]. *Infection and immunity*, 2000, 68(12): 6744-9.

567 [50] Kidd T J, Mills G, Sá - Pessoa J, et al. A *Klebsiella pneumoniae* antibiotic resistance mechanism that subdues
568 host defences and promotes virulence [J]. *Embo Molecular Medicine*, 2017, 9(4): 430.

569 A

570

571

572

573

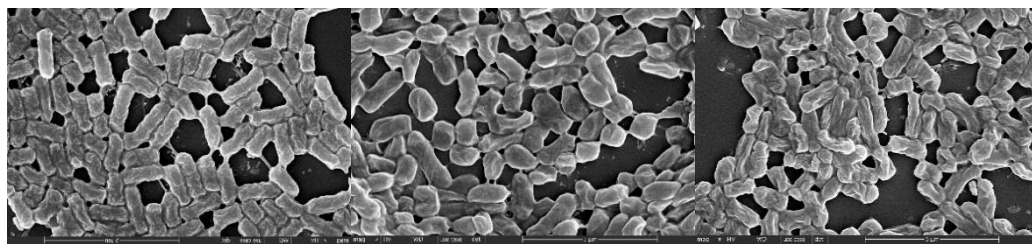
574 B

			HTH motif	
E. coli	1	MMIRERIEEKLRAAFQPVFL EVV IDESYRHNVPGSESH FKVVLV SDRFTGERFL NRHRM IYSTLAELST		70
K. pneumoniae	1	MMIREQTEAKLRAAFDPV FL EVVIDESYRHNVPGSESH FKVVLV SDRFTGERFL NRHRM IYGTLSN		70
S. Typhimurium	1	MMIREQIEEKLRTAFDPV FL EVVIDESYRHNVPGSESH FKVVLV SDRFTGERFL NRHRM IYGTLSN		70
E. coli	71	TVHAL ALH TYT IK EWEGLQDTVFASPPCRGAGSIA	105	
K. pneumoniae	71	TVHAL ALH TYT IK EWEALQDTVFASPPCRGAGSIA	105	
S. Typhimurium	71	TVHAL ALH TYT IK EWEGLQDTIFASPPCRGAGSIA	105	

575

576 C

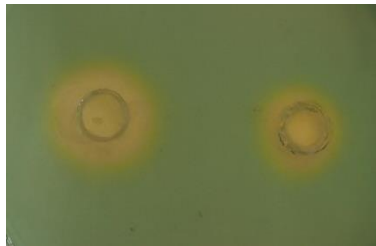
WT (in exponential phases) WT (in stationary phases) $\Delta bolA$ (in stationary phases)



577

578

579 D WT $\Delta bolA$



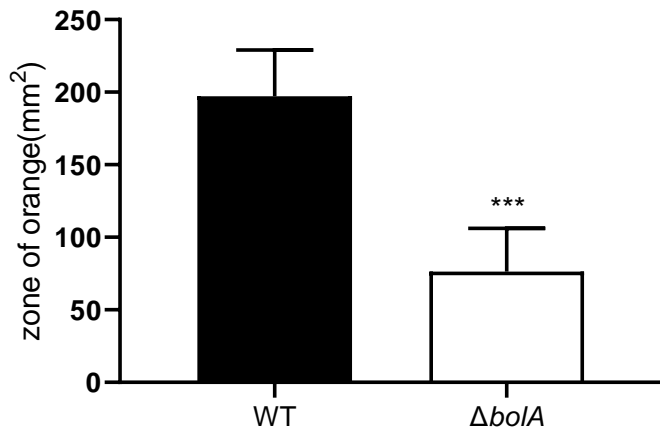
580

581

582

583

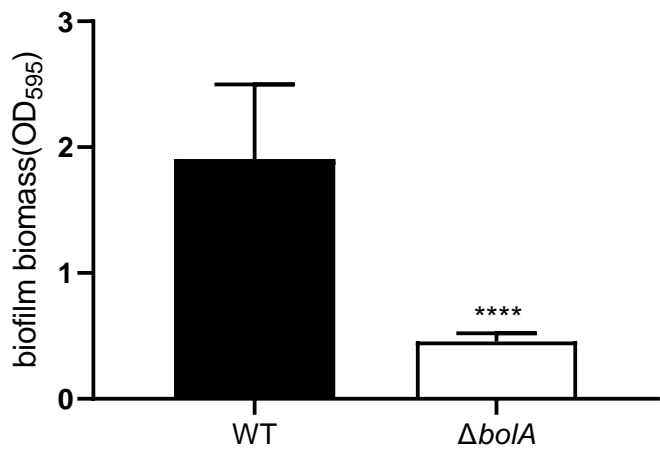
E



584

585

F

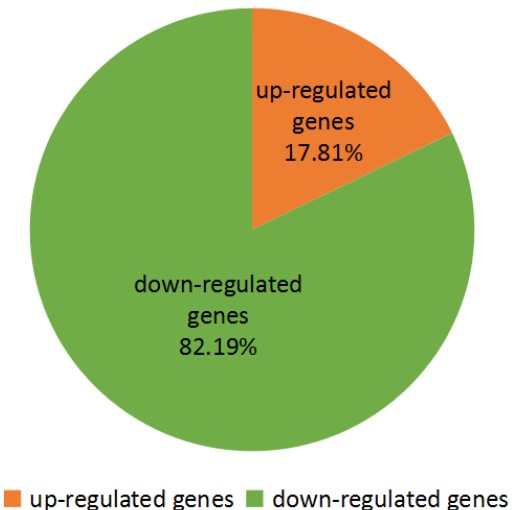


586

587 **FIG 1** BolA is essential to the cell morphology of *K. pneumoniae*. (A) A computer model of the three-dimensional (3D)

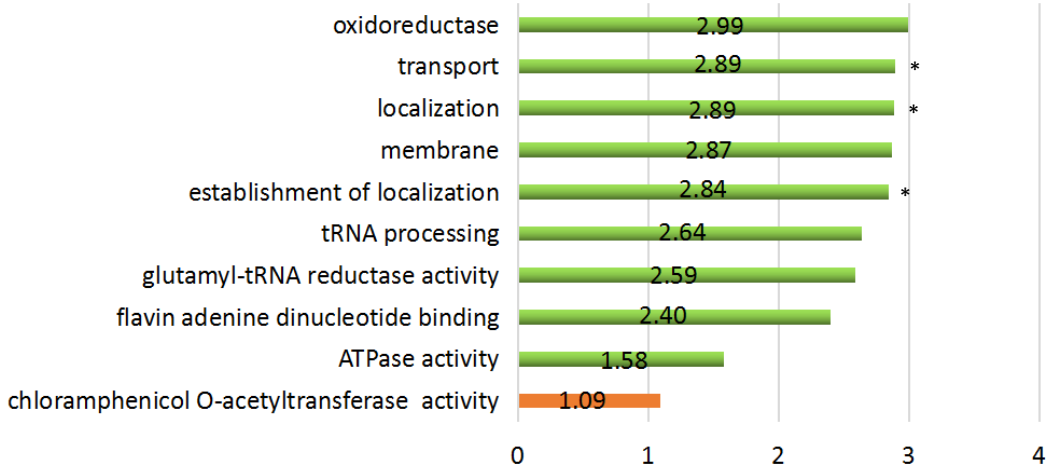
588 structure predicted from *K. pneumoniae* NTUH-K2044 BolA protein using SWISS-MODEL is presented. (B) Multiple
589 sequence alignment of BolA from *E. coli* K-12 W3110, *S. Typhimurium* SL1344 and *K. pneumoniae* NTUH-K2044
590 obtained with the DNAMAN software. The secondary structure of three BolA proteins are predicted using
591 SWISS-MODEL: in green are the β -sheets and in yellow are the α -helices. The small arrows at the top of the sequence
592 represent the amino acid of the characteristic helix to helix (HTH) FXGXXXL sequence. (C) Scanning electron
593 microscopy images of the WT and *bolA* mutant strains bacterial cells are displayed. (D) The CAS ager plate was
594 photographed after 48 h of cultivation at 28°C. (E) CAS plates were used for measure production of siderophore. The
595 larger area of the orange halo indicates that the strain has produced more siderophores and increased the capacity of
596 iron uptake. (F) The 96-well plate assay results showed *K. pneumonia* *bolA* mutant strain is defective in biofilm
597 formation. After 48 h of incubation, the biofilm biomass was measured using 0.1% of crystal violet assay, and the
598 optical density was determined at 595nm. ***, P < 0.001 by t test. ****, P<0.0001 by t test.

599 A



600

601 B



602

603 C

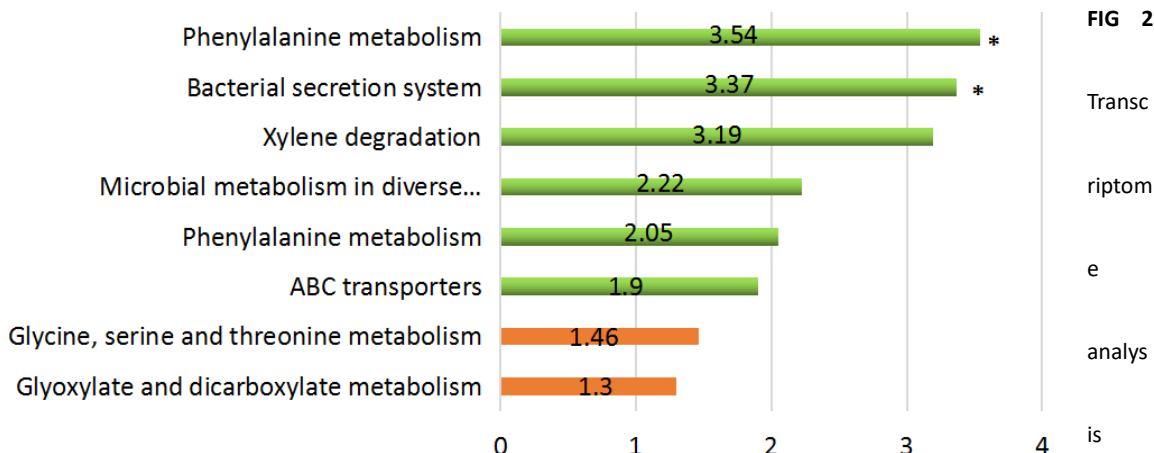


FIG 2

Transc

riptom

e

analys

is

610 between WT and Δ bolA strains. (A) Pie chart of 146 genes significantly regulated by bolA gene. The number of genes

611 significantly downregulated or upregulated are indicated in green and orange, respectively. (B) Graphical

612 representation of the gene GO enrichment analysis is in “biological process,” “cellular component,” and “molecular

613 function” categories for genes downregulated or upregulated in response to the bolA gene. *, P value associated with

614 the enrichment test was lower than 1×10^{-4} ; No asterisk indicates that the P value associated with the enrichment test

615 was between 1×10^{-2} and 1×10^{-4} . (C) Functional classification of KEGG pathway. The KEGG enrichment pathway were

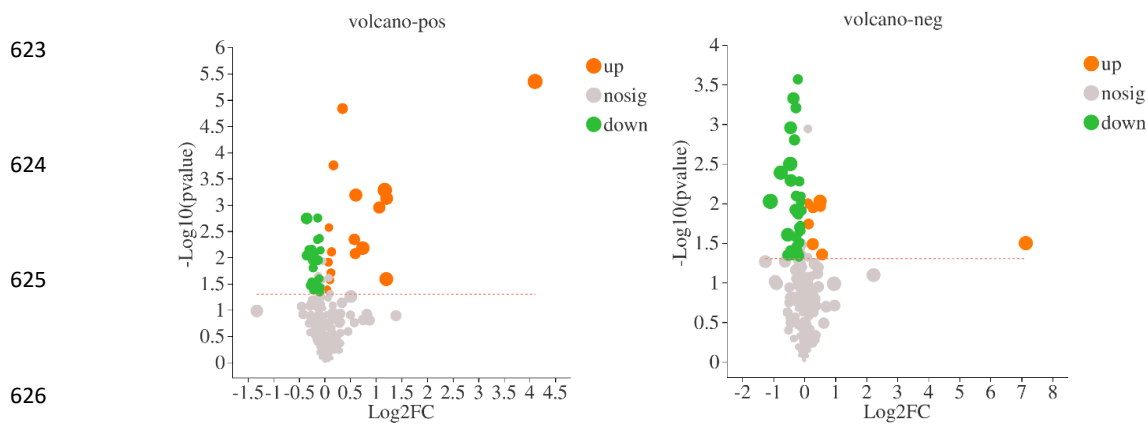
616 summarized in eight main pathways. *, P value associated with the enrichment test was lower than 0.01; No asterisk

617 indicates that the P value associated with the enrichment test was between 0.01 and 0.05. In all, the bar length
618 corresponds to the average fold change (in absolute value of the WT / Δ *bolA* ratio) of the genes significantly
619 upregulated or downregulated associated with each KEGG or GO enrichment pathways, and red graphic shows
620 upregulated pathways and green the downregulated pathways.

621 **Table 1** Differentially expressed genes involved in different pathways.

Gene	log2.Fold_change.	P value
Secretion system genes		
<i>pulK</i>	-2.9395	0.00683
<i>pulF</i>	-2.6985	0.00020409
<i>pulH</i>	-4.4938	0.0026801
<i>pulE</i>	-5.4198	1.76E-05
<i>clpV</i>	-1.6083	0.001354
<i>VgrG</i>	-3.0464	0.0017717
Biofilm genes		
<i>mhpB</i>	-4.4938	0.0026801
<i>ydeY</i>	-2.3545	0.00017415
<i>iolD</i>	-1.0834	0.00010384
Oxidoreductase genes		
<i>ulaA</i>	-4.3418	0.0046157
<i>KP1_4425</i>	-3.4869	0.00011244
<i>KP1_1420</i>	-2.4485	3.50E-06
<i>KP1_2565</i>	-1.824	0.0021176
K transport genes		
<i>kdpA</i>	-1.824	0.0021176
<i>kdpB</i>	-4.1932	8.04E-08
Iron transport genes		
<i>FhuB</i>	-2.3265	0.0027437
<i>fecD</i>	-1.0755	0.0022485
<i>FbpB</i>	-1.3265	2.57E-05
<i>afuA</i>	-2.3265	0.0027437
<i>afuB</i>	-3.9395	1.70E-06
<i>KP1_3194</i>	-1.1371	3.85E-05

622 A



633 **FIG 3 A.** Volcanic maps of differentially accumulated metabolites in WT and Δ bolA strains. Red
634 dots are upregulated metabolites, and green dots are downregulated metabolites. **B.** Results of
635 qPCR tests are showed.

636

637

638

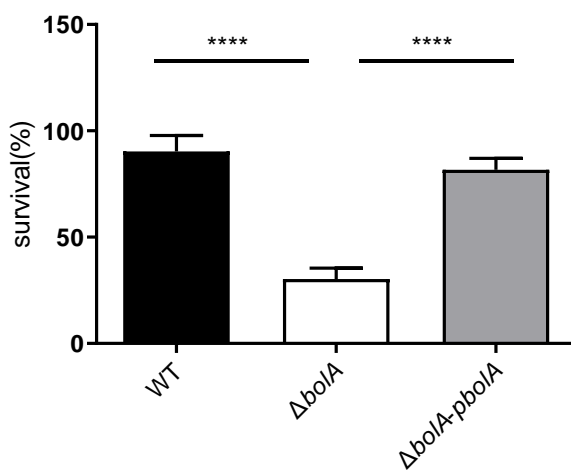
Table 2 Differentially accumulated metabolites of virulence and stress resistance.

Name	Regulated type	FC(<i>bolA</i> /WT)	VIP	P value
Agmatine	down	0.87	1.28	0.0368
Cadaverine	down	0.91	1.17	0.0045
Guanosine	down	0.94	1.16	0.0454
FAD	down	0.80	1.84	0.0016
D-Biotin	down	0.79	1.53	0.0092

639

640

A



641

642

643

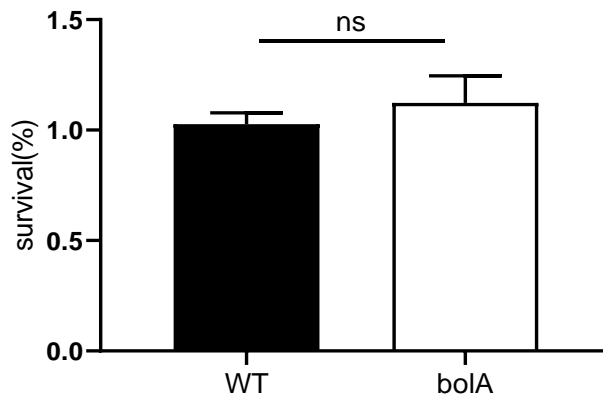
644

645

646

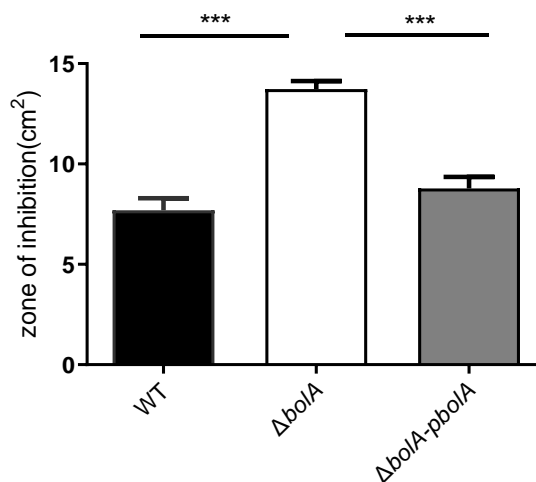
647

648 B



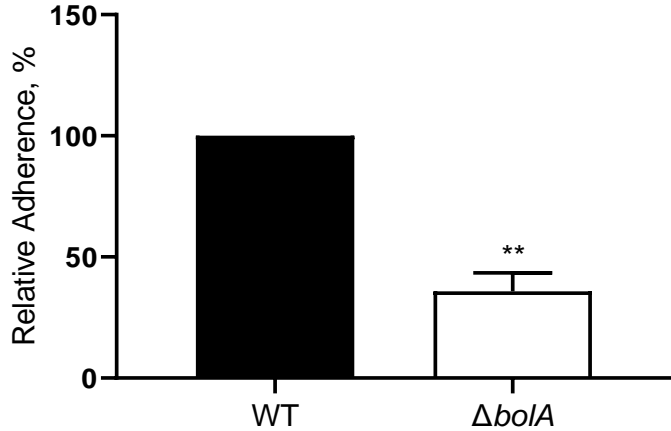
649

650 C



651

652 **FIG 4** BolA augments *K. pneumoniae* resistance to osmotic, bile and oxidative stresses. (A) The percentage of viable
653 cells were calculated by plating the appropriate dilutions on LB agar plates containing bile (1.0%). (B) The ability of
654 resistance to osmotic stress for WT, and Δ *bolA* strains were extrapolated by comparison to the numbers of viable cells
655 on LB agar plates containing NaCl (0.5 M). (C) The ability of strains to challenge hydrogen peroxide (30%) was
656 measured by disc diffusion assay. ***, Significant difference ($P<0.001$, t test), ****, Significant difference ($P<0.0001$, t
657 test), NS, not significant ($P>0.05$, t test)

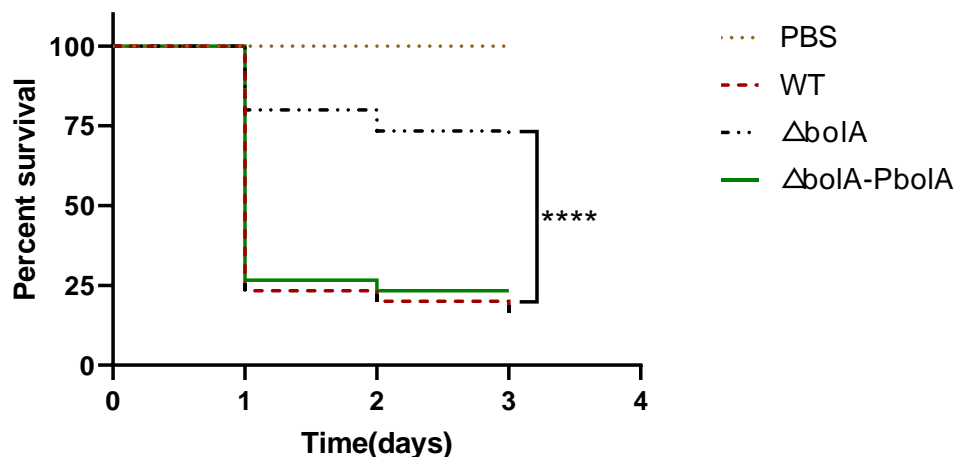


658

659 **FIG 5** Adherence of *K. pneumoniae* NTUH-K2044 WT and $\Delta bolA$ strains to HCT116 cell. The logarithmic phase *K.*
660 *pneumoniae* were added to cells of the HCT116. Next, bacteria were settled onto host cells by centrifugation at 200
661 \times g for 5 minutes, and the mixture was incubated for 1 hour, washed with PBS and then the bacteria are released
662 with Triton X-100, and plated onto LB agar for CFU counts. Rates of adherence of the *bolA* mutant strain was
663 normalized to that of WT strain (100%). **, P < 0.01 by t test.

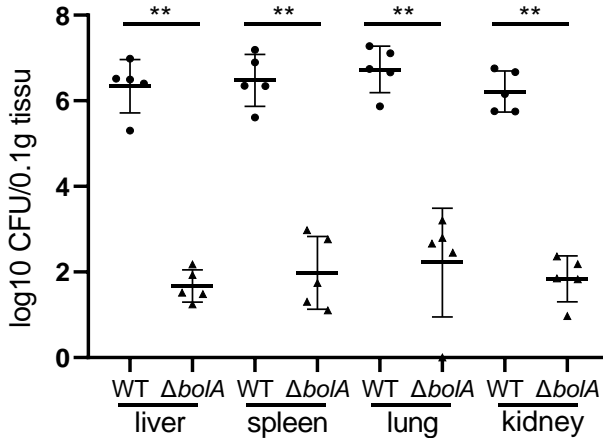
664

A



665

B



666

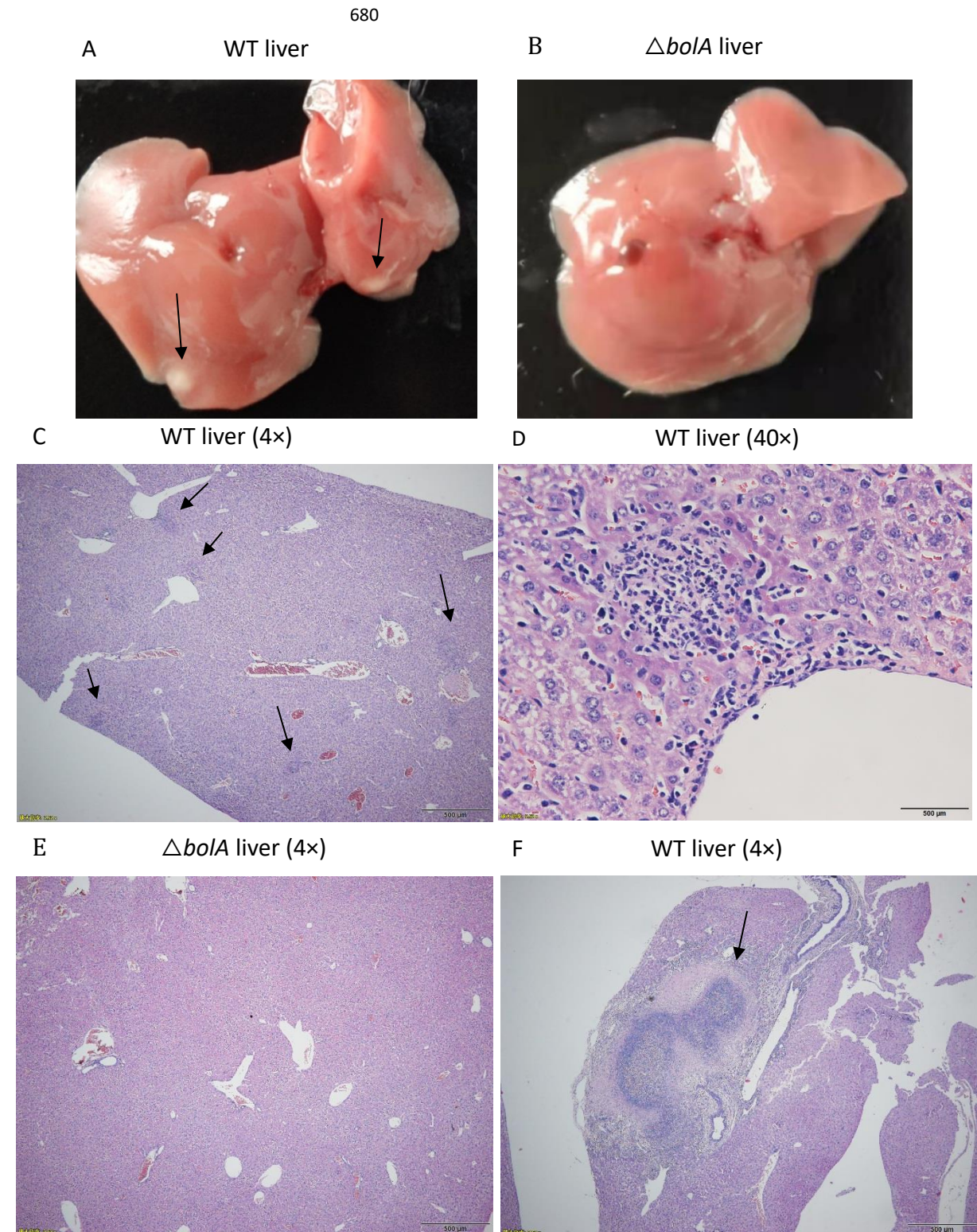
667 **FIG 6 (A)** *K. pneumoniae* *bolA* displays increased virulence in the *G. mellonella* larva infection model. Survival rate of
668 larva infected with PBS or 1×10^7 CFU of WT, Δ *bolA* and complementation strains. Larvae infected with Δ *bolA* strain
669 had enhanced survival rate compared to *K. pneumoniae* NTUH-K2044 or the complementation strains. Statistical
670 significance is examined by means of Kaplan-Meier analysis with a log-rank (Mantel-Cox) test (****, $P < 0.0001$). (B) WT
671 and Δ *bolA* strains were Intraperitoneal injection to ten-week-old female BALB/c mice (5 mice for each group) at an
672 inoculation dose of either 1×10^4 CFUs for 24 hours. The bacterial burden in liver, spleen, lung and kidney were
673 determined for each mouse by quantitative plate count at 24 hours after infection. Bacterial numbers (expressed as
674 log10 CFUs) were standardized per 0.1 gram of wet organ weight. Statistical significance is examined based on
675 unpaired nonparametric Mann-Whitney U tests (**, $P < 0.01$).

676

677

678

679



686 **FIG 7** Histopathological examination of tissues from mice. Mice were inoculated with *K. pneumoniae* WT or *bolA*
687 mutant strains (2×10^3 CFU). At 120 hours after infection, liver tissues were taken for hematoxylin-eosin staining
688 sections, and representative microscopic photos were selected for display (Fig. 7). In mice infected with the WT strain,
689 large abscesses (F, arrow) or microabscesses (C, arrow) were seen in the liver (magnification, $\times 4$); The high-power field
690 (magnification, $\times 40$) shows the microabscesses composed of inflammatory cells (D). Furthermore, in mice infected
691 with WT strain, the resected liver show significant abscesses (A, arrow); No microabscess formation was observed in
692 the liver (magnification, $\times 4$) of mice infected with *bolA* mutant strain (E), and the resected liver show no obvious
693 abscess (B).
694